

# Experience: Cross-Technology Radio Respiratory Monitoring Performance Study

Peter Hillyard  
Xandem Technology  
peter@xandem.com

Anh Luong  
Carnegie Mellon University  
anhluong@cmu.edu

Alemayehu Solomon  
Abrar  
University of Utah  
aleksol.abrar@utah.edu

Neal Patwari  
University of Utah  
and Xandem Technology  
npatwari@ece.utah.edu

Krishna Sundar  
Health Sciences Center  
University of Utah,  
krishna.sundar@hsc.utah.edu

Robert Farney  
Health Sciences Center  
University of Utah,  
robert.farney@hsc.utah.edu

Jason Burch  
Health Sciences Center  
University of Utah,  
jason.burch@hsc.utah.edu

Christina A. Porucznik  
Department of Family  
and Preventive Medicine,  
University of Utah  
School of Medicine,  
christy.porucznik@utah.edu

Sarah Hatch Pollard  
Department of Surgery,  
University of Utah  
School of Medicine,  
sarah.pollard@hsc.utah.edu

## ABSTRACT

This paper addresses the performance of systems which use commercial wireless devices to make bistatic RF channel measurements for non-contact respiration sensing. Published research has typically presented results from short controlled experiments on one system. In this paper, we deploy an extensive real-world comparative human subject study. We observe twenty patients during their overnight sleep (a total of 160 hours), during which contact sensors record ground-truth breathing data, patient position is recorded, and four different RF breathing monitoring systems simultaneously record measurements. We evaluate published methods and algorithms. We find that WiFi channel state information measurements provide the most robust respiratory rate estimates of the four RF systems tested. However, all four RF systems have periods during which RF-based breathing estimates are not reliable.

---

Permission to make digital or hard copies of all or part of this work for personal or classroom use is granted without fee provided that copies are not made or distributed for profit or commercial advantage and that copies bear this notice and the full citation on the first page. Copyrights for components of this work owned by others than ACM must be honored. Abstracting with credit is permitted. To copy otherwise, or republish, to post on servers or to redistribute to lists, requires prior specific permission and/or a fee. Request permissions from [permissions@acm.org](mailto:permissions@acm.org).

*MobiCom '18, October 29-November 2, 2018, New Delhi, India*

© 2018 Association for Computing Machinery.

ACM ISBN 978-1-4503-5903-0/18/10...\$15.00

<https://doi.org/10.1145/3241539.3241560>

## ACM Reference Format:

Peter Hillyard, Anh Luong, Alemayehu Solomon Abrar, Neal Patwari, Krishna Sundar, Robert Farney, Jason Burch, Christina A. Porucznik, and Sarah Hatch Pollard. 2018. Experience: Cross-Technology Radio Respiratory Monitoring Performance Study. In *The 24th Annual International Conference on Mobile Computing and Networking (MobiCom '18), October 29-November 2, 2018, New Delhi, India*. ACM, New York, NY, USA, 10 pages. <https://doi.org/10.1145/3241539.3241560>

## 1 INTRODUCTION

In both in-patient and in-home health care settings, respiratory monitoring plays an important role in prognosis, diagnosis, and prevention of respiratory events, disease, and death. Respiration sensing devices are typically contact-based and are wired to a monitor. Wearing a sensor can limit mobility, interrupt daily activities or disrupt sleep. There is also a risk of the sensor becoming detached. Furthermore, for patients with sensitive skin (e.g., burn patients), applying, wearing, or removing a sensor may cause significant discomfort.

Many non-contact respiration monitors have been developed to address the drawbacks of contact-based sensors. Included in this group are RF systems like Doppler and pulse radars [11], WiFi devices which measure channel state information (CSI) [31], and narrowband wireless devices which measure received signal strength (RSS) [41]. It has been shown that even the small displacement of a person's chest during respiration can change the magnitude or phase of these RF channel measurements. There is particular interest

in channel measurements from WiFi, narrowband, and ultra-wideband (UWB) devices, devices which are becoming more ubiquitous in homes and businesses with the growth of the internet of things. These devices are already being used for wireless transfer of data between devices for sensing and automation services. As these devices are transmitting data, their channel measurements can simultaneously be used for respiration monitoring.

Respiratory monitoring with WiFi, narrowband, and UWB devices have all been studied and evaluated individually. We survey RF-based, non-contact respiration monitoring. We compare measurements and devices, as well as methods for selecting the best channels from multi-channel measurements, filtering noise, detecting motion, and estimating respiration rate (RR). One common limitation is that the experimental setup heavily influences the evaluation results, and these methods have not been compared to each other. Thus it is not clear how different monitoring systems perform in comparison to another.

In this paper, we provide for the first time a side-by-side comparison of the performance of four of these RF technologies in a real-world patient study. During twenty overnight sleep studies of volunteer patients, we simultaneously measure the RF channel: the channel impulse response with a pair of UWB transceivers, channel state information with a pair of WiFi devices, and 1-dB quantized and sub-dB quantized RSS with pairs of narrowband devices. The abilities of each RF technology to estimate RR are compared to each other.

The value of the side-by-side comparison with twenty overnight studies is increased due to the number of hours of data collected, the uncontrolled nature of the studies, and the fact that many patients have disordered sleep breathing events, *e.g.* apnea and hypopnea. We collect 160 hours of data during the course of the twenty studies. During each study, the patient sleeps in a bed in a room at a sleep clinic where they are free to sleep in a given position and to move in the bed at any time. These conditions provide a very realistic environment with which to compare the RF technologies as similar conditions will likely occur in a person's home in the same uncontrolled manner. This data is public and is available at [15].

The data show that all four wireless devices can achieve as low as 0.24 breath per minute (bpm) median error during certain periods of time. We confirm that all wireless devices fail to track the RR during other significant periods of time [53]. During these failure periods, likely due to the particular arrangement of multipath components for a person's position, breathing can not be observed in the measurements. A failure period typically ends when the person moves. Particularly surprising was that even wireless devices using orders

of magnitude higher bandwidth (CIR, CSI) and multiple antenna pairs (CSI) are unable to achieve high reliability.

Overall, this study shows that WiFi CSI provides the most robust estimates of RR. We emphasize that the contribution of this paper is to provide an extensive real-world experimental setup and carefully collected data set in which four RF breathing monitoring systems and ground-truth RR data can be compared side-by-side, to our knowledge, for the first time. We hope that the results can provide direction to an active area of research and influence future systems to achieve greater performance.

## 2 RELATED WORK

RF-based respiration monitoring originated from observations that phase shifts of microwave chirp signals reflected off of a nearby, stationary person matched the person's breathing frequency [29]. Since that time, there have been significant advancements in wireless, RF-based respiration monitoring. These advancements include the type of RF channel measurements used, the availability of multidimensional measurements, motion detection methods, and methods for estimating RR. In this section, we touch on a few of these advancements and refer the reader to a more detailed survey in [16].

### 2.1 Measurement Methods

While the RF technology used to monitor respiration has evolved and expanded in capability over the last 40 years, they all leverage the same underlying physics. First, a transmitter sends a signal, and then that signal's amplitude and phase are modulated by the inhalation and exhalation of a person's chest wall. The modulated signal then arrives at a receiver which measures the changes caused by respiration. Differences in the technologies include the type of signal transmitted, the distance between the transmit and receive antenna(s), the number of transmitters and the number of receivers, and how the receiver measures the RF channel.

We categorize each technology as a monostatic or multistatic device. Multistatic devices have one or more transmit and receive antennas separated by at least 30 cm whereas monostatic devices have just one transmit antenna and one or more receive antennas but which are no more than 30 cm apart. In this paper, we focus on multistatic devices, but point to a few monostatic devices like doppler radar [6, 9–13, 18, 19, 26–28, 38, 46, 50, 58, 60, 63], frequency-modulated continuous-wave radar/sonar [2, 3, 35, 36, 43], pulse radar [20, 23, 25, 39, 40, 47, 55, 61], and pulse doppler radar [24, 56] for completeness.

In multistatic systems, a transmitter and receiver are placed so that the link line between them passes near the chest of a breathing person. The phase and amplitude of some of the

multipath components of the transmitted signal are changed as the person’s chest expands and contracts. The receiver makes a measurement of the RF channel which captures the changes in the multipath.

UWB-IR is used in both monostatic and multistatic systems. We describe in Section 5.1 how the channel impulse response (CIR) of UWB devices is used in a multistatic system to monitor respiration. This method is also implemented in past research [4, 5, 22, 45, 52]. Modern WiFi routers use orthogonal frequency division multiplexing (OFDM) to combat frequency selective fading. Recent driver modifications have given access to complex-valued signals on many subcarriers called channel state information (CSI) at the PHY layer of a WiFi enabled device [14, 59]. It has been shown that the magnitude and phase of the complex-value signal on many subcarriers [8, 30–32, 34, 44, 49, 53, 54, 57] and the RSS [1] are affected by the chest movements of a breathing person.

It has also been shown that when one or many Zigbee links are nearby a breathing person, the RSS value of the links change as a person inhales and exhales [17, 21, 41, 42, 64]. IEEE 802.15.4 transceivers often make RSS values available to the application. However, the RSS value provided is quantized with 1 dB step sizes, limiting how sensitive a link is to the small displacement of a person’s chest during breathing. An alternative system was developed to achieve sub-dB quantization step sizes [33] to provide greater sensitivity to breathing.

## 2.2 Processing and Algorithms

Different processing and algorithms are used to monitor respiration with wireless channel measurements. For example, the multistatic systems described above commonly measure multidimensional signals. For CIR, the multidimensional signal is the magnitude or phase of each tap. For CSI, the multidimensional signal is the magnitude or phase of each subcarrier on each MIMO link. For RSS, the multidimensional signal is each frequency channel on which received signal strength is measured. In this section, we refer to an individual tap, subcarrier, or channel in the multidimensional signal as a stream. It is common however for some streams to have a higher signal-to-noise ratio (SNR) than other streams. For reliable respiration monitoring, selecting the best stream(s) is necessary.

During respiration monitoring, RF devices measure very small displacements of a person’s chest during respiration. Larger motion like walking, moving an arm or leg, or even muscle twitches can induce very large changes in RF measurements. During periods of motion, it is very difficult to recover the breathing signal as it is overwhelmed by effects of motion. Many motion detection algorithms have been

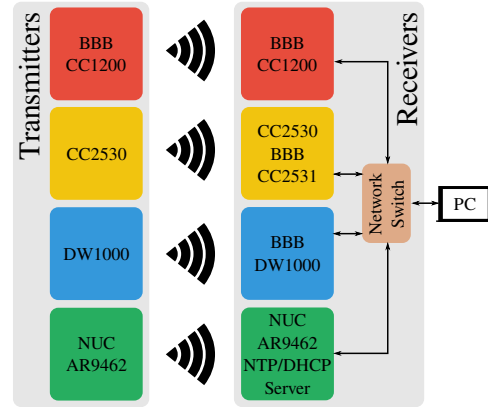


**Figure 1: The components of the RF testbed. The transmitter components are contained in the box on the left, and the receiver components are contained in the box on the right.**

developed to flag RF measurements as happening during motion events.

A common way to evaluate the performance of a respiration monitoring system is to estimate the RR of a person and compare the estimate to ground truth. Frequency domain and time domain methods have been developed to estimate the RR. Prior to RR estimation, the signals are commonly filtered to either remove high frequency content, DC offset, or both.

## 3 EQUIPMENT

In this section, we describe the testbed used to study four different RF-based respiratory monitoring systems. We also describe the polysomnography equipment used to collect ground truth data.

### 3.1 RF System Testbed

In this section, we discuss the design of the four different systems representing the current state-of-the-art in non-contact multistatic RF respiratory monitoring including UWB-IR, WiFi CSI, Zigbee RSS, and sub-1 dB quantized RSS. The components of this system are discussed in the following sections and are shown in Fig. 1.

**Sub-dB RSS:** A CC1200 radio with a WA5VJB Log Periodic 400-1000 MHz antenna is placed in both the transmitter and receiver box. The CC1200 transmitter and receiver are controlled with a BeagleBone Black (BBB). The transmitter sends a 900 MHz continuous wave and the receiver measures sub-1 dB quantized RSS measurements as described in [33]. The measurements are stored on the receiver’s BeagleBone Black. We refer to this measurement system as SUB. The CC1200 provides one power measurement at a sampling rate of  $f_s^{sub} = 487.5$  Hz. For this paper, the signal is

downsampled by 30 by averaging non-overlapping chunks of measurements.

**Zigbee RSS:** One CC2530 transceiver with a WA5VJB Log Periodic 900-2600 MHz antenna is placed in each of the transmitter and receiver boxes. A logging CC2531 radio is attached to a BBB to save the RSS measured between the two transceivers. The transceivers use TDMA to take turns transmitting while looping through all sixteen 2.4 GHz Zigbee channels. We refer to this measurement system as RSS. We will distinguish between the system and the measurement when necessary. The RSS measurements are saved at a sampling rate of  $f_s^{rss} = 4.5$  Hz.

**WiFi CSI:** We replace the existing WiFi card in an Intel NUC D54250WYK with an Atheros AR9462. We use the CSI tool developed in [59] and modify the kernel driver to operate in the WiFi 5 GHz band. Two WA5VJB Log Periodic 2.11-11.0 GHz antennas are attached to the WiFi card to enable  $2 \times 2$  MIMO. One modified Intel NUC serves as the access point and is placed in the transmitter box. Another modified Intel NUC serves as the client and is placed in the receiver box. The client pings the access point and records CSI for 114 subcarriers on each MIMO link. We refer to this measurement system as CSI. We will distinguish between the system and the measurement when necessary. A complex-valued CSI measurement on 114 subcarriers from  $2 \times 2$  MIMO is saved at a sampling rate of  $f_s^{csi} = 9.9$  Hz.

**UWB-IR:** A Decawave EVB1000 is placed in the transmitter box. The transmitter sends UWB packets on a channel that occupies 3.77 - 4.24 GHz. A second EVB1000 in the receiver box measures the CIR and sends the complex-valued CIR taps to a BBB. Both the transmitter and receiver use the PCB UWB antenna provided with the EVB1000. We refer to this measurement system as CIR. We will distinguish between the system and the measurement when necessary. A complex-valued CIR measurement is sent from the Decawave RX to a BBB at a sampling rate of  $f_s^{cir} = 18.9$  Hz.

**Network:** The RF devices in the receiver box are attached to the a NetGear 5-port switch and are time synchronized using NTP with the Intel NUC as the NTP server. The Intel NUC is also a DHCP server. The devices are housed in separate boxes (see Fig. 2).

**Polysomnography:** Patients who come for a sleep study are dressed with a number of sensors including respiratory impedance plethysmography (RIP) belts around the chest and abdomen, and a thermistor and nasal cannula sensor in their nose. These sensors are plugged into an amplifier, and their measurements are read into Natus SleepWorks Software [37] for visualization. The data collected are exported as an EDF and converted to ASCII [51] to be processed offline.

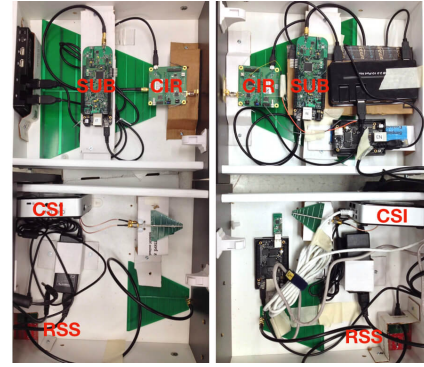


Figure 2: RF transmitters (left) and receivers (right) enclosed in the drawers of a bedside dresser.

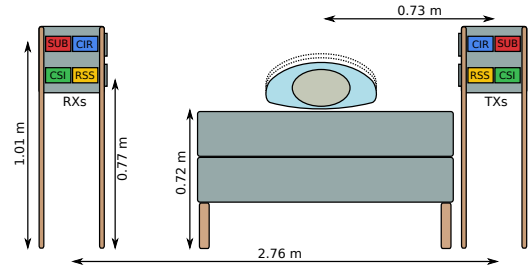
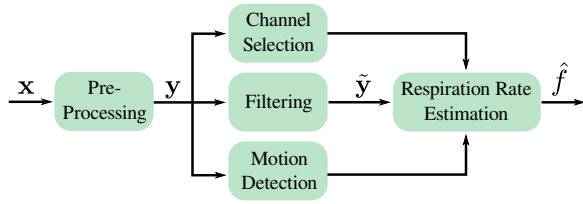


Figure 3: Position of the RF sensor and the patient's bed during each clinical study. Relevant heights and distances are included.

## 4 CLINICAL STUDY

In our clinical study, 20 patients, who were already scheduled for a regular 8 h sleep study, were asked to participate in a breathing monitoring experiment. Willing participants read and signed a consent form for IRB 00084836. Thereafter, the RF testbed was turned on and then positioned so that the link line between transmitter and receiver was perpendicular to and on top of the person's chest as shown in Fig. 3. The patient was then outfitted with polysomnograph sensors and, once in bed, the sleep study began. During the study, registered polysomnographic technologists annotated the polysomnograph data with the time and duration of pertinent events related to sleep. These annotations were reviewed a second and third time by other technicians and physicians.

The events recorded by the sleep technicians include limb movements, arousals, obstructive hypopnea and apnea, central apnea, sleep stage, and sleeping position. These events are important for rating sleep quality and diagnosing sleep disorders. The polysomnography and RF data and annotated events from all twenty studies have been anonymized and made publicly available for future researchers' use [15]. Height, weight, gender, and age statistics are provided in [16].



**Figure 4: Breathing monitoring blocks to perform signal processing on RF measurements, to select the best streams from a multidimensional signal, to estimate RR  $\hat{f}$ , and to detect motion periods.**

## 5 METHODS

In this section, we describe a variety of methods that are commonly used in RR estimation. These methods can be categorized into the blocks shown in Fig. 4. The multidimensional channel measurement  $\mathbf{x}$  is fed into a pre-processing block. A series of filters in the filter block attenuates undesired frequency content. Streams of the multidimensional measurements are then selected to be used in respiratory rate estimation. A motion detection block is used to ignore RR estimates during motion. The methods that we evaluate are from previously published methods.

### 5.1 Pre-Processing

Each RF technology requires unique signal processing algorithms for each RF system in order to extract a breathing signal. A detailed description of all of the pre-processing methods used in this paper are provided in [16].

### 5.2 Stream Selection

Destructive and constructive interference of multipath components results in some streams being more sensitive to respiration than others. Stream selection is used to remove unwanted streams, or weight the stream based on some metric for RR estimation. The stream selection algorithms presented in previous research do not perform well with the data we collected. As such, we implement new stream selection algorithms for each RF channel measurement. A detailed description of stream selection methods used in this paper are provided in [16].

### 5.3 Signal Filtering

The initial processing performed for each RF technology yields a measurement vector  $\mathbf{y}$ . A person’s chest moving during inhalation and exhalation cause sinusoidal changes to  $\mathbf{y}$ . We filter these measurements to remove unwanted high and low frequency components in the measurements.

On average, the respiratory rate of a healthy adult at rest is 14 bpm [48], and can vary from 12-15 bpm [7]. We consider that higher frequency components in the signal are caused

by motion other than respiration or by noise which we desire to filter out. We create a fifth-order Butterworth low-pass filter with a cutoff frequency of 0.4 Hz to attenuate high frequency signals. The Butterworth filter’s flat frequency response in the passband is desirable since it does not amplify any specific frequencies in the passband.

After running  $\mathbf{y}$  through a low-pass filter, we run the measurements through a high-pass filter to obtain a zero-mean signal. This is a necessary step when computing the power spectral density (PSD) of a noisy, finite length signal since the DC component can overwhelm the power of lower amplitude sinusoidal components. We discuss the PSD in Section 5.4. The high-pass filter is a fifth-order Butterworth filter with a cutoff frequency of 0.1 Hz. We denote the measurement after the low and high-pass filter as  $\tilde{\mathbf{y}}$ .

### 5.4 Respiratory Rate Estimation

The processed and filtered RF measurements have a sinusoidal component when the person is breathing. To estimate the respiratory rate, we first compute the average PSD using a 10 - 30 s window of measurements [41]. The frequency at which the PSD is maximum is the estimated RR. We denote this estimated RR as  $\hat{f}_{psd}$  Hz. In this paper, we use a 30 s window of measurements and compute the PSD between  $f_{min} = 0.1$  Hz and  $f_{max} = 0.4$  Hz with a step size of  $f_{step} = 0.002$  Hz.  $f_{min}$  and  $f_{max}$  are set to account for a range of breathing rates for a resting healthy adult. A new  $\hat{f}$  estimate is produced every 5 s.

### 5.5 Ground Truth Respiration Rate

In each polysomnography study, the patient is monitored using a variety of sensors including respiratory inductance plethysmography (RIP) belts around the chest and abdomen, and a thermocouple and nasal pressure sensor placed in the nose. The RIP belts measure the chest and abdomen expanding and contracting during breathing. The thermocouple measures changes in the temperature related to inspiration and exhalation while the nasal pressure sensor measures changes in pressure related to the same.

One measurement from each of these four sensors form the measurement vector  $\mathbf{y}^{poly} \in \mathbb{R}^4$  and are sampled at  $f_s^{poly} = 25$  Hz. The measurements are then sent through a low-pass and high-pass filter as was described in Section 5.3 to form the vector  $\tilde{\mathbf{y}}^{poly}$ . The ground-truth RR is then estimated using the PSD estimation solution described in Section 5.4.

### 5.6 Motion Detection

Motion detectors provide a way to flag periods of time when the RR estimate is not reliable. The motion detectors we implement in this paper have been developed in previous works and are described in more detail in [16]. For reference,

**Table 1: The median and 95th percentile  $e$  for each RF technology.**

RF Tech	Median $e$	95th pctl. $e$
CIR	1.32	11.88
CSI	0.60	11.88
RSS	1.56	12.84
SUB	3.36	13.08

we implement a moving average based detector (MABD) [62], a moving variance based detector (MVBD) [62], an average variance energy detector (AVE) [30], a flat spectrum detector (FSD) [2], and a combination of moving average and variance (MAVBD). In this paper, we evaluate the usefulness of motion detection algorithms for long-term RR monitoring by comparing performance when motion detection is and is not used. When motion detection is used, we also compare how each method performs against the other. When motion is detected, we ignore the RR estimate by letting  $\hat{f} = NaN$ .

## 6 RESULTS

In this section, we compare the RR estimation as a function of wireless device and motion detection method. Additional comparisons of stream selection, sleep position, and RR estimation method are presented in [16].

### 6.1 Performance Metrics

The performance of each RF technology are compared using the absolute difference between the true and estimated RR. This metric is formalized as

$$e = 60 \cdot |f_{gt} - \hat{f}| \quad (1)$$

where  $f_{gt}$  is the ground truth frequency in Hz and  $e$  is in bpm. The polysomnography and each RF technology have a different sampling frequency, and so  $e$  is computed using the  $f_{gt}$  and  $\hat{f}$  measured at the closest points in time. When a motion detection algorithm is used,  $\hat{f} = NaN$  and so we do not compute  $e$ .

### 6.2 Overall RR Estimation Results

In this section, we compare the RR estimation error of all four wireless devices using the PSD RR estimation method and disabling the motion detection block. In Fig. 5 we observe the CDF of  $e$  over all twenty studies. The differences between the CDFs are summarized in Table 1 which shows the median and 95th percentile  $e$  of each RF technology. An important observation we make is that there is a difference between CDFs when we compare each RF technology. CSI achieves the lowest median  $e$ , two to five times lower than the median  $e$  for CIR, RSS, and SUB. Stated differently, when a person is breathing at  $\geq 12$  bpm, the median  $e$  when using CSI will

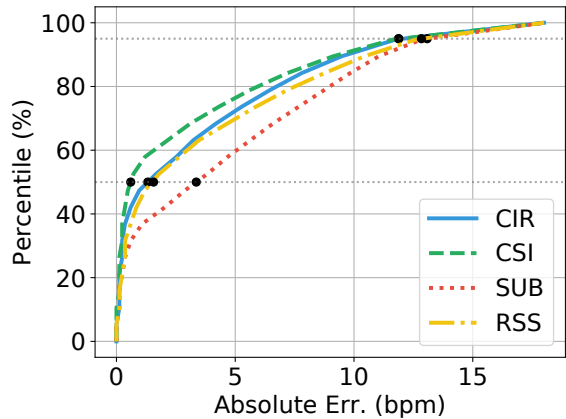


**Figure 5: CDF of  $e$  over all 20 studies when stream select is enabled. A PSD method is used but motion detection is bypassed.**

be within  $\geq 95\%$  of the true RR. Why CSI achieves a lower median  $e$  compared to the other wireless devices, and CIR in particular which uses the most bandwidth, could be a function of CSI’s frequency diversity, making use of antenna diversity by measuring a MIMO instead of SISO channel, the larger number of streams used for RR estimation, and/or its coherence bandwidth. These and other possibilities could be investigated to provide a more theoretical reasoning for CSI performing the best out of the four RF devices.

However, these results don’t tell the full story. While CSI achieves the lowest median  $e$ , the CDFs show that all four RF devices are all able to achieve very low RR estimation errors. For CSI, 56% of the estimates are less than 1 bpm, 47% for CIR, 44% for RSS, and 36% for SUB. All technologies can achieve low RR errors, but they all vary in how often the RR estimate is accurate. The other side to this story is that there is a significant number of RR estimates which are unreliable for all four RF devices. In the following sections, we offer observations of why the RR estimate can be so unreliable.

### 6.3 Motion Detection Effect on RR Estimates

So far, we have not included the output of a motion detection method while estimating RR. Motion periods can result in large changes in the channel measurements which overwhelm the small changes caused by respiration. Motion events can, in turn, cause large errors in the RR estimation. This can be seen in Fig. 6. In this figure, we observe that there are a few RR estimate errors above 1.5 bpm. The number of high error estimates after a motion event is greater for RSS and SUB than for CIR and CSI. But all RF technologies are affected by motion to some degree.

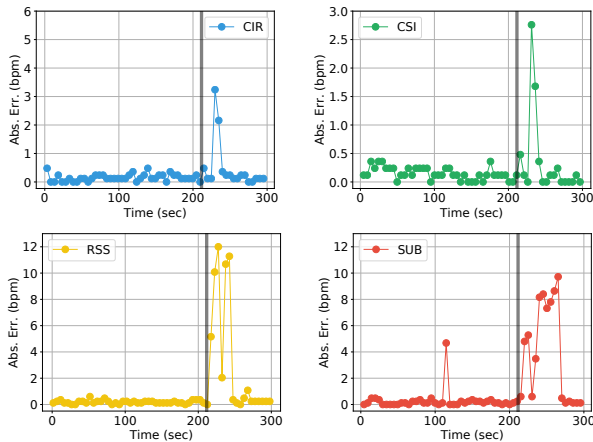


**Figure 6: A five minute interval showing the absolute error achieved by each technology when no motion detection algorithm is used. The gray band shows a period when motion occurred.**

To negate the periods of large  $e$  due to motion, we compare the five motion detection methods described in Section 5.6. Each motion detection algorithm is evaluated one at a time. We compare the motion detection performance using the median  $e$  achieved over all 20 studies and the percent of RR estimates that are ignored because of detected motion. These metrics provide a way to judge each algorithm’s ability to remove the large RR estimate errors caused by motion and the ability to remove only estimates that were made during periods of motion. The results of this evaluation is shown in Fig. 7. We observe that all of the motion detectors improve the median  $e$  when compared to the case where no motion detection is used. The MABD tends to lower the median  $e$  the most for each RF technology. However, the percent of RR estimates removed when using MABD tends to increase as well. From our observations, there is on average one motion event every 5 min. Motion events during sleep do not last any more than 30 s. So over the course of an 8 h study, there should be 10% of the time when we are not estimating a respiratory rate. We use this percentage as a benchmark for the motion detectors. Additional sensing devices would have been needed to be attached to the patient during the sleep study to get a more accurate ground truth for motion. Removing less than 10% of the estimates means that more RR estimates could be affected by motion and thus increase the median  $e$ . Alternatively, removing more than 10% of the RR estimates means that we are not estimating RR rate even though there is no motion.

With this tradeoff in mind, we observe that the performance of motion detector varies with the RF technology. For SUB, the MABD reduces the median  $e$  by 0.4 bpm and removes 12% of the RR estimates. For RSS, MVBD lowers the

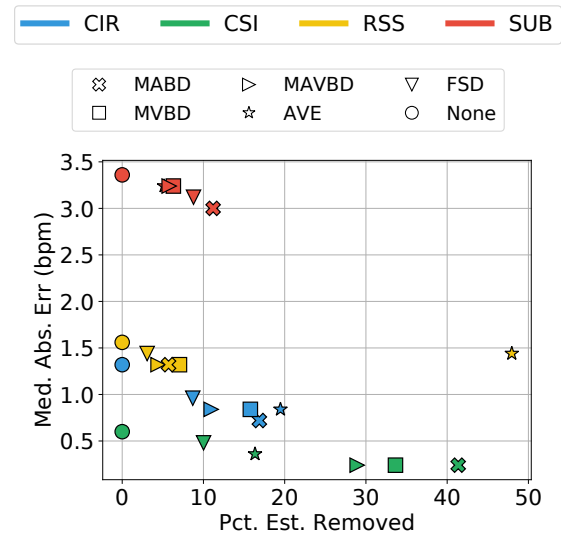


**Figure 7: The median  $e$  and % RRs ignored because of detected motion vs. motion detection method and RF technology.**

median  $e$  by 0.3 bpm and removes the most RR estimates. For CIR, MAVDB lowers the median  $e$  by 0.5 bpm and removes 11% of the RR estimates. Lastly for CSI, FSD comes the closest to 10% RR estimates removed and lowers the median  $e$  by 0.1 bpm. We note that the thresholds we chose for each motion detection algorithm plays a role in the percent of RR estimates removed. Additional evaluation would need to be performed to show a more complete representation of how each motion detection algorithm could perform with different thresholds. However, for the purpose of this paper, it is sufficient to say that applying a motion detection algorithm can lower the median  $e$  by removing RR estimates that were made during a period motion. No one motion detection method was definitively the best in terms of balancing a reduced median  $e$  and ignoring true periods of motion.

#### 6.4 RR Estimation Robustness

Unlike the controlled and short studies conducted in prior research, the patients monitored during the sleep studies were not instructed to lie in a certain position for a certain amount of time. Veritably, patients would move during the study and could change their sleeping position at will. One reality with wireless RF respiratory monitoring is that even slight changes in a person’s position will alter the fading characteristics of each stream of an RF device. When the multipath components add destructively at the receiver, the respiration signal will be hidden in noise or will be nonexistent. When this is the case for a large percentage of selected streams, RR estimation is very difficult.

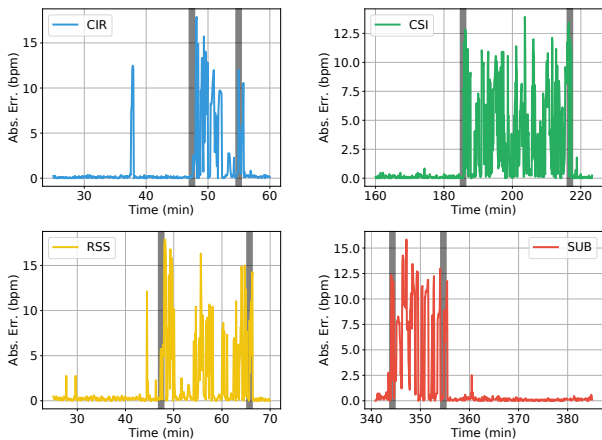


**Figure 8: The absolute error  $e$  vs. method during several minutes of different study periods. The gray bands indicate two times when the patient moved during the period shown.**

**Table 2: Median  $e$  (bpm) for each RF technology for errors shown in Fig. 8**

Motion Events	CIR	CSI	RSS	SUB
Before	0.12	0.12	0.24	0.24
Between	2.22	3.12	1.0	7.38
After	0.24	0.12	0.12	0.12

To demonstrate this reality, we plot in Fig. 8 different sections of time from a patient study when each RF device has periods of low and then high RR estimation error that are related to periods of motion. The gray bands in Fig. 8 indicate the two times the patient moved during the window of errors shown. All four RF technologies have periods where the  $e$  is much lower than 1 bpm. When the patient moves, the errors are higher and appear to be more uniformly distributed. The patient moves again after some time, and the error drops back down below 1 bpm error. The median absolute error before the first motion event, between the two motion events, and after the last motion event for each RF technology is summarized in Table 2. We see that the median RR estimates for all RF technologies are well below 1 bpm error before and after the motion events. In fact, there is very little difference in estimation error when fading conditions are favorable for each RF technology. We also observe that every RF technology suffers from very unreliable RR estimates during some periods. When the fading conditions are not favorable, the median error increases for all RF technologies. This result is surprising for CSI and CIR. Despite having more diversity from using multiple antennas and/or operating with a large bandwidth, CSI and CIR are not able to reliably track RR at

all times. CSI and CIR suffer just like the RSS-based technologies from being in unfavorable fading conditions for periods of time.

An argument could be made that there is no difference in RR estimation among the technologies, conditioned on having favorable fading conditions. Consequently, COTS devices that only measure RSS on narrow channel bandwidths could be just as useful in respiration monitoring as a WiFi or UWB device that use much wider channel bandwidths. The difference is that CSI appears to be in a favorable fading condition the greatest amount of time. One question to ask is, is it possible to increase the amount of time that favorable fading exists? For example, achieving accurate RR estimates may hinge on introducing spatial diversity with more devices or antennas thereby increasing the number of streams with high respiratory signal SNR.

## 7 CONCLUSION

In this paper, we developed a respiratory monitoring testbed containing four different RF devices to simultaneously measure the wireless channel. Included were WiFi devices that measured CSI, UWB radios that measured CIR, and two narrowband radios that measured 1-dB quantized and sub-dB quantized RSS. The testbed, placed in a sleep study room, collected channel measurements all night during twenty polysomnographies. The four RF technologies and motion detection were then compared using the error in the RR estimate as a metric.

We found that CSI measurements resulted in the lowest median absolute error in RR estimates compared to CIR, RSS, and SUB. Yet, even with multiple antennas and/or large bandwidth, CSI and CIR failed to reliably track the respiratory rate over the long term just like the RSS and SUB which did not have the same points of diversity. In our tests, we found that there was no significant difference in performance between motion detection algorithms. This study showed that many RF-based systems can perform respiratory monitoring equally reliably at times, but also that each system could be improved to overcome periods of time when the fading conditions are not favorable.

## ACKNOWLEDGMENT

Research reported in this publication was supported in part by the National Institute on Drug Abuse of the National Institutes of Health under Award Number #DA041960 and by the U. S. Army Research Office grant #69215CS. The content is solely the responsibility of the authors and does not necessarily represent the official views of the NIH or the ARO.



## REFERENCES

- [1] H. Abdelnasser, K. A. Harras, and M. Youssef. Ubibreathe: A ubiquitous non-invasive WiFi-based breathing estimator. In *Proc. of the 16th ACM Int. Symp. on Mobile Ad Hoc Networking and Computing, MobiHoc '15*, pages 277–286, 2015.
- [2] F. Adib, H. Mao, Z. Kabelac, D. Katabi, and R. C. Miller. Smart homes that monitor breathing and heart rate. In *Proc. of the 33rd Annu. ACM Conf. on Human Factors in Computing Syst., CHI '15*, pages 837–846, 2015.
- [3] L. Anitori, A. de Jong, and F. Nennie. FMCW radar for life-sign detection. In *2009 IEEE Radar Conf.*, pages 1–6, May 2009.
- [4] M. Baboli, O. Boric-Lubecke, and V. Lubecke. A new algorithm for detection of heart and respiration rate with UWB signals. In *2012 Annual Intl. Conf. of the IEEE Engineering in Medicine and Biology Society*, pages 3947–3950, Aug 2012.
- [5] M. Baboli, A. Sharafi, A. Ahmadian, and M. Nambakhsh. An accurate and robust algorithm for detection of heart and respiration rates using an impulse based UWB signal. In *2009 Int. Conf. on Biomedical and Pharmaceutical Eng.*, pages 1–4, Dec 2009.
- [6] T. Ballal, R. B. Shouldice, C. Heneghan, and A. Zhu. Breathing rate estimation from a non-contact biosensor using an adaptive IIR notch filter. In *2012 IEEE Topical Conf. on Biomedical Wireless Technologies, Networks, and Sensing Syst. (BioWireless)*, pages 5–8, Jan 2012.
- [7] K. E. Barrett, S. Boitano, S. M. Barman, and H. L. Brooks. Overview respiratory physiology. In *Ganong's Review of Medical Physiology, 24e*, New York, NY, 2012. The McGraw-Hill Companies.
- [8] C. Chen, Y. Han, Y. Chen, H. Q. Lai, F. Zhang, B. Wang, and K. J. R. Liu. TR-BREATH: Time-reversal breathing rate estimation and detection. *IEEE Trans. on Biomedical Eng.*, PP(99):1–1, 2017.
- [9] K. M. Chen, D. Misra, H. Wang, H. R. Chuang, and E. Postow. An X-band microwave life-detection system. *IEEE Trans. on Biomedical Engineering*, BME-33(7):697–701, July 1986.
- [10] D. Dei, G. Grazzini, G. Luzi, M. Pieraccini, C. Atzeni, S. Boncinelli, G. Camiciottoli, W. Castellani, M. Marsili, and J. Lo Dico. Non-contact detection of breathing using a microwave sensor. *Sensors*, 9(4):2574–2585, 2009.
- [11] A. D. Droitcour, O. Boric-Lubecke, and G. T. A. Kovacs. Signal-to-noise ratio in Doppler radar system for heart and respiratory rate measurements. *IEEE Trans. on Microwave Theory and Techniques*, 57(10):2498–2507, Oct 2009.
- [12] A. D. Droitcour, T. B. Seto, B. K. Park, S. Yamada, A. Vergara, C. E. Hourani, T. Shing, A. Yuen, V. M. Lubecke, and O. Boric-Lubecke. Non-contact respiratory rate measurement validation for hospitalized patients. In *2009 Annu. Int. Conf. of the IEEE Eng. in Medicine and Biology Soc.*, pages 4812–4815, Sept 2009.
- [13] C. Graichen, J. Ashe, M. Ganesh, and L. Yu. Unobtrusive vital signs monitoring with range-controlled radar. In *2012 IEEE Signal Proc. in Medicine and Biology Symp. (SPMB)*, Dec 2012.
- [14] D. Halperin, W. Hu, A. Sheth, and D. Wetherall. Tool release: Gathering 802.11n traces with channel state information. *ACM SIGCOMM CCR*, 41(1):53, Jan. 2011.
- [15] Hillyard. RF respiration monitoring dataverse, 2018. <https://doi.org/10.7910/DVN/X7AYXQ>.
- [16] P. Hillyard, A. Luong, A. S. Abrar, N. Patwari, K. Sundar, R. Farney, J. Burch, C. A. Porucznik, and S. H. Pollard. Comparing respiratory monitoring performance of commercial wireless devices, 2018. arXiv:1807.06767.
- [17] R. Hostettler, O. Kaltiokallio, H. Yigitler, S. Särkkä, and R. Jäntti. Rss-based respiratory rate monitoring using periodic gaussian processes and kalman filtering. In *2017 25th European Signal Processing Conf. (EUSIPCO)*, pages 256–260, Aug 2017.
- [18] W. Hu, H. Zhang, Z. Zhao, Y. Wang, and X. Wang. Real-time remote vital sign detection using a portable Doppler sensor system. In *2014 IEEE Sensors Applicat. Symp. (SAS)*, pages 89–93, Feb 2014.
- [19] W. Hu, Z. Zhao, Y. Wang, H. Zhang, and F. Lin. Noncontact accurate measurement of cardiopulmonary activity using a compact quadrature Doppler radar sensor. *IEEE Trans. on Biomedical Engineering*, 61(3):725–735, March 2014.
- [20] I. Immoreev and T. H. Tao. UWB radar for patient monitoring. *IEEE Aerospace and Electronic Syst. Mag.*, 23(11):11–18, Nov 2008.
- [21] O. Kaltiokallio, H. Yigitler, R. Jäntti, and N. Patwari. Non-invasive respiration rate monitoring using a single COTS TX-RX pair. In *Proc. of the 13th Int. Symp. on Inform. Process. in Sensor Networks (IPSN '14)*, pages 59–69, April 2014.
- [22] Y. Kilic, H. Wymeersch, A. Meijerink, M. J. Buntum, and W. G. Scanlon. Device-free person detection and ranging in UWB networks. *IEEE J. of Select. Topics in Signal Processing*, 8(1):43–54, Feb 2014.
- [23] J. C. Y. Lai, Y. Xu, E. Gunawan, E. C. P. Chua, A. Maskooki, Y. L. Guan, K. S. Low, C. B. Soh, and C. L. Poh. Wireless sensing of human respiratory parameters by low-power ultrawideband impulse radio radar. *IEEE Trans. on Instrumentation and Measurement*, 60(3):928–938, March 2011.
- [24] A. Lazaro, D. Girbau, and R. Villarino. Analysis of vital signs monitoring using an IR-UWB radar. In *Progress In Electromagnetics Research*, volume 100, pages 265–284, 2010.
- [25] M. Leib, W. Menzel, B. Schleicher, and H. Schumacher. Vital signs monitoring with a UWB radar based on a correlation receiver. In *Proc. of the 4th European Conf. on Antennas and Propagation*, pages 1–5, April 2010.
- [26] C. Li, J. Ling, J. Li, and J. Lin. Accurate Doppler radar noncontact vital sign detection using the relax algorithm. *IEEE Trans. on Instrumentation and Measurement*, 59(3):687–695, March 2010.
- [27] P. Li and D. c. Wang. A quadrature Doppler radar system for sensing human respiration and heart rates. In *IEEE 10th Int. Conf. on Signal Processing Proc.*, pages 2235–2238, Oct 2010.
- [28] W. Li, B. Tan, and R. J. Piechocki. Non-contact breathing detection using passive radar. In *2016 IEEE Int. Conf. on Commun. (ICC)*, pages 1–6, May 2016.
- [29] J. C. Lin. Noninvasive microwave measurement of respiration. *Proceedings of the IEEE*, 63(10):1530–1530, Oct 1975.
- [30] J. Liu, Y. Wang, Y. Chen, J. Yang, X. Chen, and J. Cheng. Tracking vital signs during sleep leveraging off-the-shelf WiFi. In *Proc. of the 16th ACM Int. Symp. on Mobile Ad Hoc Networking and Computing, MobiHoc '15*, pages 267–276, 2015.
- [31] X. Liu, J. Cao, S. Tang, and J. Wen. Wi-sleep: Contactless sleep monitoring via WiFi signals. In *2014 IEEE Real-Time Sys. Symp.*, pages 346–355, Dec 2014.
- [32] X. Liu, J. Cao, S. Tang, J. Wen, and P. Guo. Contactless respiration monitoring via off-the-shelf WiFi devices. *IEEE Trans. Mobile Comput.*, 15(10):2466–2479, Oct 2016.
- [33] A. Luong, A. S. Abrar, T. Schmid, and N. Patwari. RSS step size: 1 dB is not enough! In *Proc. of the 3rd Workshop on Hot Topics in Wireless, HotWireless '16*, pages 17–21, 2016.
- [34] J. Ma, Y. Wang, H. Wang, Y. Wang, and D. Zhang. When can we detect human respiration with commodity WiFi devices? In *Proc. of the 2016 ACM Int. Joint Conf. on Pervasive and Ubiquitous Computing: Adjunct, UbiComp '16*, pages 325–328, 2016.
- [35] R. Nandakumar, S. Gollakota, and N. Watson. Contactless sleep apnea detection on smartphones. In *Proceedings of the 13th Annual International Conference on Mobile Systems, Applications, and Services, MobiSys '15*, pages 45–57, 2015.
- [36] R. Nandakumar, A. Takakuwa, T. Kohno, and S. Gollakota. Covertband: Activity information leakage using music. *Proc. ACM Interact. Mob. Wearable Ubiquitous Technol.*, 1(3):87:1–87:24, Sept. 2017.

- [37] Natus. Sleep works software, 2017. <http://www.natus.com>.
- [38] P. Nguyen, X. Zhang, A. Halbower, and T. Vu. Continuous and fine-grained breathing volume monitoring from afar using wireless signals. In *IEEE INFOCOM 2016 - The 35th Annual IEEE Int. Conf. on Computer Commun.*, pages 1–9, April 2016.
- [39] V. Nguyen, A. Q. Javaid, and M. A. Weitnauer. Harmonic path (HAPA) algorithm for non-contact vital signs monitoring with IR-UWB radar. In *2013 IEEE Biomedical Circuits and Syst. Conf. (BioCAS)*, Oct 2013.
- [40] G. Ossberger, T. Buchegger, E. Schimback, A. Stelzer, and R. Weigel. Non-invasive respiratory movement detection and monitoring of hidden humans using ultra wideband pulse radar. In *2004 Intl. Workshop on Ultra Wideband Systems*, pages 395–399, May 2004.
- [41] N. Patwari, L. Brewer, Q. Tate, O. Kaltiokallio, and M. Bocca. Breathfinding: A wireless network that monitors and locates breathing in a home. *IEEE J. Sel. Topics Signal Process.*, 8(1):30–42, Feb 2014.
- [42] N. Patwari, J. Wilson, S. Ananthanarayanan, S. K. Kasera, and D. R. Westenskow. Monitoring breathing via signal strength in wireless networks. *IEEE Trans. Mobile Comput.*, 13(8):1774–1786, Aug 2014.
- [43] Z. Peng, J. M. Muñoz-Ferreras, Y. Tang, C. Liu, R. Gómez-García, L. Ran, and C. Li. A portable fmcw interferometry radar with programmable low-if architecture for localization, isar imaging, and vital sign tracking. *IEEE Trans. on Microwave Theory and Techniques*, 65(4):1334–1344, April 2017.
- [44] R. Ravichandran, E. Saba, K. Y. Chen, M. Goel, S. Gupta, and S. N. Patel. Wibreathe: Estimating respiration rate using wireless signals in natural settings in the home. In *2015 IEEE Int. Conf. on Pervasive Computing and Commun. (PerCom)*, pages 131–139, March 2015.
- [45] N. V. Rivera, S. Venkatesh, C. Anderson, and R. M. Buehrer. Multi-target estimation of heart and respiration rates using ultra wideband sensors. In *2006 14th European Signal Processing Conf.*, pages 1–6, Sept 2006.
- [46] J. Salmi, O. Luukkonen, and V. Koivunen. Continuous wave radar based vital sign estimation: Modeling and experiments. In *2012 IEEE Radar Conf.*, pages 0564–0569, May 2012.
- [47] J. Salmi and A. F. Molisch. Propagation parameter estimation, modeling and measurements for ultrawideband MIMO radar. *IEEE Trans. on Antennas and Propagation*, 59(11):4257–4267, Nov 2011.
- [48] P. Sebel. *Respiration, the breath of life*. Torstar Books, 1985.
- [49] J. Shang and J. Wu. Fine-grained vital signs estimation using commercial WiFi devices. In *Proc. of the 8th Wireless of the Students, by the Students, and for the Students Workshop, S3*, pages 30–32, 2016.
- [50] J. Tu, T. Hwang, and J. Lin. Respiration rate measurement under 1-D body motion using single continuous-wave Doppler radar vital sign detection system. *IEEE Trans. on Microwave Theory and Techniques*, 64(6):1937–1946, June 2016.
- [51] T. van Beelen. EDF to ASCII converter, 2017. <https://www.teuniz.net/edf2ascii/>.
- [52] S. Venkatesh, C. R. Anderson, N. V. Rivera, and R. M. Buehrer. Implementation and analysis of respiration-rate estimation using impulse-based UWB. In *MILCOM 2005 - 2005 IEEE Military Commun. Conf.*, volume 5, pages 3314–3320, Oct 2005.
- [53] H. Wang, D. Zhang, J. Ma, Y. Wang, Y. Wang, D. Wu, T. Gu, and B. Xie. Human respiration detection with commodity WiFi devices: Do user location and body orientation matter? In *Proc. of the 2016 ACM Int. Joint Conf. on Pervasive and Ubiquitous Computing, UbiComp '16*, pages 25–36, 2016.
- [54] X. Wang, C. Yang, and S. Mao. Phasebeat: Exploiting csi phase data for vital sign monitoring with commodity WiFi devices. In *2017 IEEE 37th Int. Conf. on Distributed Computing Syst. (ICDCS)*, pages 1230–1239, June 2017.
- [55] Y. Wang, Q. Liu, and A. E. Fathy. Simultaneous localization and respiration detection of multiple people using low cost UWB biometric pulse Doppler radar sensor. In *2012 IEEE/MTT-S Int. Microwave Symp. Digest*, pages 1–3, June 2012.
- [56] D. T. Wisland, K. Granhaug, J. R. Pley, N. Andersen, S. Støa, and H. A. Hjortland. Remote monitoring of vital signs using a CMOS UWB radar transceiver. In *2016 14th IEEE Intl. New Circuits and Systems Conf. (NEWCAS)*, pages 1–4, June 2016.
- [57] C. Wu, Z. Yang, Z. Zhou, X. Liu, Y. Liu, and J. Cao. Non-invasive detection of moving and stationary human with WiFi. *IEEE J. on Select. Areas in Commun.*, 33(11):2329–2342, Nov 2015.
- [58] Z. Xia and Y. Zhang. Dual-carrier noncontact vital sign detection with a noise suppression scheme based on phase-locked loop. *IEEE Trans. on Microwave Theory and Techniques*, 64(11):4003–4011, Nov 2016.
- [59] Y. Xie, Z. Li, and M. Li. Precise power delay profiling with commodity WiFi. In *Proc. of the 21st Annu. Int. Conf. on Mobile Computing and Networking, MobiCom '15*, pages 53–64, 2015.
- [60] Z. Yang, P. H. Pathak, Y. Zeng, X. Liran, and P. Mohapatra. Vital sign and sleep monitoring using millimeter wave. *ACM Trans. Sen. Netw.*, 13(2):14:1–14:32, Apr. 2017.
- [61] P. R. Yifan Chen. Human respiration rate estimation using ultrawideband distributed cognitive radar system. *Int. J. of Automation and Computing*, 5(4):325, 2008.
- [62] M. Youssef, M. Mah, and A. Agrawala. Challenges: Device-free passive localization for wireless environments. In *Proceedings of the 13th Annual ACM Intl. Conf. on Mobile Computing and Networking, MobiCom '07*, pages 222–229, 2007.
- [63] H. Zhao, H. Hong, L. Sun, Y. Li, C. Li, and X. Zhu. Noncontact physiological dynamics detection using low-power digital-IF Doppler radar. *IEEE Trans. on Instrumentation and Measurement*, 66(7):1780–1788, July 2017.
- [64] Y. Zhao, J. Ashe, and T. Yu. Respiration monitoring using a wireless network with space and frequency diversities. In *2016 IEEE Int. Conf. on Consumer Electronics (ICCE)*, pages 474–477, Jan 2016.